



---

*Research article*

## Numerical investigation of fractional-order unsteady natural convective radiating flow of nanofluid in a vertical channel

M. Hamid<sup>1,\*</sup>, T. Zubair<sup>1</sup>, M. Usman<sup>2,3,4,\*</sup> and R. U. Haq<sup>5</sup>

<sup>1</sup> School of Mathematical Sciences, Peking University, Beijing 100871, China

<sup>2</sup> BIC-ESAT, College of Engineering, Peking University, Beijing 100871, China

<sup>3</sup> State Key Laboratory for Turbulence and Complex Systems, Department of Mechanics and Engineering Science, Peking University, Beijing 100871, China

<sup>4</sup> Institute of Ocean Research, Peking University, Beijing 100871, China

<sup>5</sup> Department of Electrical Engineering, Bahria University, Islamabad Campus, Islamabad 44000, Pakistan

\* **Correspondence:** Email: mhamid@pku.edu.cn, mmusmans@hotmail.com.

**Abstract:** In the current article, we analyzed the unsteady natural convection with the help of fractional approach. Firstly, the unsteady natural convection radiating flow in an open ended vertical channel beside the magnetic effects. We assumed the channel is stationary with non-uniform temperature. Secondly, we utilized a fractional calculus approach for the constitutive relationship of a fluid model. The modeled problem is transformed into nondimensional form via viable non-dimensional variables. In order to investigate the numerical solutions of non-dimensional system of partial differential equations finite difference approach coupled with Crank Nicolson method is developed and successfully applied. The beauty of Crank Nicolson finite difference scheme is, this scheme is unconditionally stable. A very careful survey of literate witnesses that this scheme has never been reported in the literary for fluid problems. The physical changes are discussed with the help of graphics. The expression for both velocity field and temperature distribution has been made via said scheme. A comprehensive discussion about the influence of various related dimensionless parameters upon the flow properties disclosed our work. It is observed that velocity field decreases as enhancing the magnetic field effects. Heat transfer enhanced as enhancing the nanoparticle volume fraction parameter. Velocity field and heat transfer shows the dominant behavior for the case of  $Cu$ -based nanofluid as compare to  $Al_2O_3$  based nanofluid. Comparative study also included to show the accuracy of the proposed finite difference scheme. It is to be highlighted that the proposed scheme is very efficient and well-matched to

---

investigate the solutions of modeled problem and can be extended to diversify problems of physical nature.

**Keywords:** finite difference method; fractional calculus; nanofluid; magnetic effects; thermal radiation

**Mathematics Subject Classification:** 34A08

---

## 1. Introduction

The exponential growth of natural convection radiating flow has gained a considerable attention in the developing research area. Many numerical, theoretical and experimental investigation has been made for natural convection radiating flow of viscous fluids in vertical cylinders, in a channel and over an infinite plate. Fujii et al. [1] experimentally analyzed the natural-convection transfer of heat from the external surface of a vertical cylinder to liquids. Fujii and Imura [2] provided an experimental investigation about concerning natural-convection heat transfer from a plate with arbitrary inclination. In their study they restricted the boundary layer flow to 2D (two-dimensional). Ezzat, [3] examined the heat transport and MHD thermoelectric flow of non-Newtonian fluid with fractional derivative. Arshad et al. [4] studied the natural convection heat transfer from a bounded assembly of thin non-horizontal cylinders. Their work was purely reported an experimental study of natural convection. Eldabe et al. [5] numerically examines the influence of viscous dissipation on free convection heat and mass transfer of MHD non-Newtonian fluid flow through a porous medium. Rubbab et al. [6] analyzed the natural convection flow near a vertical plate. Ellahi [7] analytically examined the impacts of temperature dependent viscosity and MHD flow of nanofluid in a pipe. Natural convection flow along an isothermal vertical flat plate with temperature dependent viscosity and heat generation examined by Molla et al. [8]. Ezzat et al. [9] described the heat and mass transfer through a MHD time-dependent viscoelastic fluid enclosed by infinite vertical plates. The simulations are performed via Laplace-transform method (LTM) and behavior of concentration, temperature, velocity, electric and induced magnetic field distributions have been analyzed via set of graphs. Sheri and Thumma [10] studied the heat transfer enhancement in MHD free convection flow over vertical plate utilizing nanofluids. The readers are referred to see [11–15] for some recent literature related to combined analysis of MHD natural convection in different fluid problems.

The field of fluid mechanics gained a worthy consecration after the Choi contribution [16–17]. He was the pioneer who worked on improvement of the thermal conductivity of the fluids. According to his idea there is an appropriate quantity of nanoparticles inside the traditional fluids. He named the term as nanofluids. The experimental outcomes reconfirm that thermal properties of traditional fluids can be enhanced by using Choi idea. After this ground breaking innovation this domain gained a significant importance and a lot of work reported in the literature. Dinarvand et al. [18] studied the Buongiorno's model for double-diffusive mixed convective stagnation-point flow of a nanofluid considering diffusiophoresis effect of binary base fluid. Three dimensional mesoscopic simulation of magnetic field effect on natural convection of nanofluid studied by Sheikholeslami and Ellahi [19]. Sheikholeslami and Ganji [20] analyzed the nanofluid convective heat transfer. They used both numerical and analytical approaches to investigate the said nanofluid model. Usman et al. [21] used an analytical technique (DTM) to investigate the unsteady nanofluid flow and heat transfer. Hassan

et al. [22] conducted a model study for both magnetic and non-magnetic particles in nanofluid over a wedge and presented a comparative analysis. Mohyud-Din [23] reported the influence of Marangoni convection and thermal radiation effects on CNT-Water flow of nanofluid. A least squares technique is adopted to present the analysis for said flow model while findings are asserted with the help of graphical sets. The thermal boundary thickness and temperature both enhanced while increase the nanoparticle friction. It is reported that the velocity of the fluid is decreased for both kinds of CNTs. Hamid et al. [24] examined the heat and mass transport for MHD time-dependent flow of nanofluid in the presence of natural convection, thermal radiation and heat sink/source. The solution of reduced nonlinear PDEs is obtained via Crank-Nicolson finite difference scheme. The small values of time with increasing Reynolds number an enhanced velocity distribution is perceived. The temperature profile is dropped for Biot numbers while enhanced for higher values of Reynolds, Brownian motion, thermophoresis, and heat source numbers. An inclusive study associated to nanofluids via various aspects can be find in [25–29].

Previously, the fractional calculus theory has gained extensive concern because of its large range of applications in various areas of engineering and physics [30]. The fractional calculus has been exploited with ample success in the description of complex dynamics such as wave, viscoelastic and relaxation behaviors. In fractional calculus due to development of operator a straightforward technique for presenting fractional derivatives into models of linear viscous is to change the first derivative in the constitutive equation of the natural convection model with an  $\alpha \in (0,1)$  order fractional derivative. The fractional calculus provides some noticeable contributions in relating frequent technological and scientific situations such as capacitor theory, viscoelasticity, electrical circuits, electro-analytical chemistry, diffusion and neurology [31–32]. Different methods have been proposed by various authors to tackle non-linearity of fractional differential equations [33–36]. Although there is a comprehensive research literature available on the fluid flows, many mathematical models employed the fractional calculus to solve a variety of applied fluid flow problems. We are citing some recent literate related to said domain [37–40].

The present work is an extension of [40] in which we analyzed the unsteady natural convection radiating flow in an open ended vertical channel beside the magnetic effects. The channel is stationary with non-uniform temperature. We utilized a fractional calculus approach for the constitutive relationship of a fluid model. The finite difference approach [41] along with Crank Nicolson method [42] has been successfully applied [13,28]. The careful literature survey witnesses that this scheme has never been reported in the literary. The physical changes are discussed with the help of graphical plots. The expression for both velocity field and temperature distribution has been made via said scheme. Finally, a detailed discussion about the influence of various related dimensionless parameters upon the flow properties disclosed our work.

## 2. Mathematical and geometrical analysis

Let us examine the effects of heat transfer of unsteady, one dimensional, naturally convected, and viscous flow. It is also consider that the fluid is enclosed between two non-uniform, stagnant and parallel walls separated by distance  $d$ ,  $x$  and  $y$  – axis are considered along flow direction and normal to flow direction respectively. Assume that the temperature of wall and fluid has constant value  $T_\infty$ . Furthermore, temperature of plate reserved at  $y = 0$  and  $t > 0$  is preserved as initial temperature  $T_\infty$  and natural convection current is produced because the temperature of wall kept at

$y = d$  is raised up and is considered  $T_w$ . Applied Magnetic field is considered constant and electric field is pondered as zero. The induced magnetic field is neglected due to small Reynolds number. In view of Boussinesq approximation, flow can be explained with the help of following partial differential equations [40]

$$\frac{\partial u}{\partial t} = \nu_{nf} \frac{\partial^2 u}{\partial y^2} + \frac{g}{\rho_{nf}} \beta_{nf} (T - T_\infty) + \frac{1}{\rho_{nf}} (\mathbf{J} \times \mathbf{B})_x, \quad (1)$$

$$(\rho C_P)_{nf} \frac{\partial T}{\partial t} = k_{nf} \frac{\partial^2 T}{\partial y^2} - \frac{\partial q_r}{\partial y}, \quad (2)$$

where  $u(y, t)$ ,  $T(y, t)$ ,  $g$ ,  $\nu_{nf}$ ,  $\rho_{nf}$ ,  $\beta_{nf}$ ,  $\sigma_{nf}$ ,  $(C_P)_{nf}$ ,  $k_{nf}$ ,  $\mathbf{J}$  are the velocity along  $x$ -axis, temperature along  $x$ -axis, gravitational acceleration, kinematics viscosity for nano-fluid, density of nano-fluid, heat transfer constant for nano-fluid, electrical conductivity for nano-fluid, heat capacity of for nano-fluid, thermal conductivity for nano-fluid, current density respectively and also defined as [12].

$$\nu_{nf} = \frac{\mu_{nf}}{\rho_{nf}}, \mu_{nf} = \frac{\mu_f}{(1-\phi)^{2.5}}, \rho_{nf} = \rho_f \left( (1-\phi) + \phi \frac{\rho_s}{\rho_f} \right), \quad (3a)$$

$$(\rho c_p)_{nf} = (1-\phi)(\rho c_p)_f + \phi(\rho c_p)_s, (\rho \beta)_{nf} = (1-\phi)(\rho \beta)_f + \phi(\rho \beta)_s, \quad (3b)$$

where  $\rho_f$ ,  $\rho_s$ ,  $\beta_f$ ,  $\beta_s$ ,  $\mu_{nf}$ ,  $\mu_f$  and  $\phi$  are density of fluid, density of solid particle, heat transfer constant for fluid, heat transfer constant for solid particle, viscosity of nano-fluid, viscosity of fluid, viscosity of solid particle and solid volume fraction respectively.

The value of current density is

$$\mathbf{J} = \sigma_{nf} (E + \mathbf{V} \times \mathbf{B}), \quad (4)$$

where  $E$  is the electric field. Cogley et al. [43], shows that [30]:

$$\frac{\partial q_r}{\partial y} = 4(T - T_\infty) \int_0^\infty k_{\lambda_w} \left( \frac{de_{b\lambda}}{dt} \right)_w d\lambda, \quad (5)$$

where  $k_\lambda$ ,  $e_{b\lambda}$ ,  $w$  are the absorption coefficient, plank function and value at the wall  $y = d$ . Substituting the values from Eqs (4) and (5) into Eqs (1) and (2), once obtained

$$\frac{\partial u}{\partial t} = \nu_{nf} \frac{\partial^2 u}{\partial y^2} + \frac{g}{\rho_{nf}} \beta_{nf} (T - T_\infty) - \frac{\sigma B_0^2}{\rho_{nf}} u, \quad (6)$$

$$(\rho c_P)_{nf} \frac{\partial T}{\partial t} = k_{nf} \frac{\partial^2 T}{\partial y^2} - 4(T - T_\infty)I, \quad (7)$$

where  $I = \int_0^\infty k_{\lambda_w} \left( \frac{de_{b\lambda}}{dt} \right)_w d\lambda$ .

The associated initial and boundary condition of problem (6)–(7) are

$$u(y, 0) = u(0, t) = u(1, t) = 0,$$

$$T(y, 0) = T(0, t) = T_\infty, T(1, t) = T_w.$$

Introducing the transformation for Eqs (6) and (7) is given by

$$u = \frac{\nu_f}{d} U, t = \frac{d^2}{\nu_f} t^*, y = dY, T - T_\infty = (T_w - T_\infty) T^*. \quad (8)$$

Using (3) and (8), once obtained

$$\left[ (1 - \phi) + \phi \frac{\rho_s}{\rho_f} \right] \frac{\partial U}{\partial t^*} = \frac{1}{(1 - \phi)^{2.5}} \frac{\partial^2 U}{\partial Y^2} + GrT^* \left[ (1 - \phi) + \phi \frac{(\rho\beta)_s}{(\rho\beta)_f} \right] - M^2 U, \quad (9)$$

$$\left[ (1 - \phi) + \phi \frac{(\rho\beta)_s}{(\rho\beta)_f} \right] Pr \frac{\partial T^*}{\partial t^*} = \frac{k_{nf}}{k_f} \frac{\partial^2 T^*}{\partial Y^2} - RT^*, \quad y \in [0, 1], t \geq 0, \quad (10)$$

where  $Gr, M^2, Pr$  and  $R$  are the Grashof number, Hartmann number, Prandtl number and radiation parameter and is defined as

$$Gr = \frac{g\beta_f(T_w - T_\infty)d^3}{\nu_f^2}, M^2 = \frac{\sigma B_0^2 d^2}{\mu_f}, Pr = \frac{\mu_f(c_p)_f}{k_f}, R = \frac{4Id^2}{k_f}.$$

After applying the above transformations boundary condition reduces as:

$$u(y, 0) = 0, u(0, t) = 0, u(1, t) = 0,$$

$$T(y, 0) = 0, T(0, t) = 0, T(1, t) = 1.$$

The Caputo time fractional form of Eqs (9) and (10) are explained as

$$\left[ (1 - \phi) + \phi \frac{\rho_s}{\rho_f} \right] D_t^\alpha u(y, t) = \frac{1}{(1 - \phi)^{2.5}} \frac{\partial^2 u}{\partial y^2} + GrT \left[ (1 - \phi) + \phi \frac{(\rho\beta)_s}{(\rho\beta)_f} \right] - M^2 u, \quad (11)$$

$$\left[ (1 - \phi) + \phi \frac{(\rho\beta)_s}{(\rho\beta)_f} \right] Pr D_t^\alpha T(y, t) = \frac{k_{nf}}{k_f} \frac{\partial^2 T}{\partial y^2} - RT, \quad (12)$$

$$\text{where } D_t^\alpha T(y, t) \begin{cases} \frac{1}{\Gamma(1-\alpha)} \int_0^t \frac{1}{(t-\tau)^\alpha} \frac{\partial T(y, \tau)}{\partial \tau} d\tau, & 0 < \alpha < 1, \\ \frac{\partial T(y, t)}{\partial t}, & \alpha = 1. \end{cases}$$

### 3. Finite difference scheme

In this section, we introduce the well-known Crank-Nicholson finite difference scheme for the numerical solution of the following fractional partial differential equations:

$$\frac{\rho_{nf}}{\rho_f} \frac{\partial^\alpha}{\partial t^\alpha} u(y, t) = \frac{1}{(1 - \phi)^{2.5}} \frac{\partial^2}{\partial y^2} u(y, t) - M^2 u(y, t) + \frac{(\rho\beta)_{nf}}{(\rho\beta)_f} GrT(y, t), \quad (13)$$

$$\frac{(\rho c_p)_{nf}}{(\rho c_p)_f} Pr \frac{\partial^\alpha}{\partial t^\alpha} T(y, t) = \frac{k_{nf}}{k_f} \frac{\partial^2}{\partial y^2} T(y, t) - RT(y, t), \quad (14)$$

along with the boundary conditions associated with (13–14). In above  $0 < \alpha \leq 1$  is Caputo derivative of fractional order. Consider that the above fractional-order system has sufficiently smooth and has a unique. Assume that  $x_j = jh, 0 \leq j \leq M$  with  $Mh = 1$  and  $t_n = n\tau, 0 \leq n \leq N$ . Here  $h$  and  $\tau$  indicates the space and time step length,  $M$  and  $N$  are represents the number of grids point. Fractional order derivate can discretize as [41]:

$$D_t^\alpha Q(y, t) = \frac{1}{\tau^\alpha \Gamma(2 - \alpha)} \left[ Q_j^{n+1} - Q_j^n + \sum_{i=1}^n (Q_j^{n-i+1} - Q_j^{n-i}) ((i+1)^{1-\alpha} - i^{1-\alpha}) \right] + O(\tau),$$

and the second order derivative using Crank-Nicholson idea can be discretize as under:

$$\frac{\partial^2}{\partial y^2} Q(y, t) = \frac{1}{2h^2} [(Q_{j+1}^{n+1} - 2Q_j^{n+1} + Q_{j-1}^{n+1}) + (Q_{j+1}^n - 2Q_j^n + Q_{j-1}^n)] + O(h^2).$$

Using the above discretize formulas, system (12–13) takes the following form:

$$\begin{aligned}
 & -\omega_{\tilde{u}} \tilde{u}_{j+1}^{n+1} + (\vartheta_{\tilde{u}} + 2\omega_{\tilde{u}}) \tilde{u}_j^{n+1} - \omega_{\tilde{u}} \tilde{u}_{j-1}^{n+1} = \omega_{\tilde{u}} \tilde{u}_{j+1}^n + (\vartheta_{\tilde{u}} - 2\omega_{\tilde{u}} - M^2) \tilde{u}_j^n + \omega_{\tilde{u}} \tilde{u}_{j-1}^n + \\
 & \frac{(\rho\beta)_{nf}}{(\rho\beta)_f} Gr \tilde{T}_j^n - \vartheta_{\tilde{u}} \sum_{i=1}^n (\tilde{u}_j^{n-i+1} - \tilde{u}_j^{n-i}) b_i, \\
 & -\omega_{\tilde{T}} \tilde{T}_{j+1}^{n+1} + (\vartheta_{\tilde{T}} + 2\omega_{\tilde{T}}) \tilde{T}_j^{n+1} - \omega_{\tilde{T}} \tilde{T}_{j-1}^{n+1} = \omega_{\tilde{T}} \tilde{T}_{j+1}^n + (\vartheta_{\tilde{T}} - 2\omega_{\tilde{T}} - R) \tilde{T}_j^n + \omega_{\tilde{T}} \tilde{T}_{j-1}^n - \\
 & \vartheta_{\tilde{T}} \sum_{i=1}^n (\tilde{T}_j^{n-i+1} - \tilde{T}_j^{n-i}) b_i,
 \end{aligned}$$

$$\text{where } \omega_{\tilde{u}} = \frac{1}{(1-\phi)^{2.5}} \frac{1}{2h^2}, \vartheta_{\tilde{u}} = \frac{\rho_{nf}}{\rho_f} \frac{1}{\tau^{\alpha} \Gamma(2-\alpha)}, \omega_{\tilde{T}} = \frac{k_{nf}}{k_f} \frac{1}{2h^2}, \vartheta_{\tilde{T}} = \frac{(\rho c_p)_{nf}}{(\rho c_p)_f} \frac{Pr}{\tau^{\alpha} \Gamma(2-\alpha)},$$

$$b_i = ((i+1)^{1-\alpha} - i^{1-\alpha}).$$

$$\mathbf{A}_1 \mathbf{v}^1 = \mathbf{B} \mathbf{v}^0 + \frac{(\rho\beta)_{nf}}{(\rho\beta)_f} Gr \mathbf{C} \mathbf{v}^0,$$

for  $n \geq 1$ ,

$$\mathbf{A}_{n+1} \mathbf{v}^{n+1} = \mathbf{B}_{n+1} \mathbf{v}^n + \mathbf{s}_1^{n+1} \mathbf{v}^n + \mathbf{s}_2^{n+1} \mathbf{v}^{n-1} + \dots + \mathbf{s}_n^{n+1} \mathbf{v}^1 + \mathbf{b}^{n+1} \mathbf{v}^0 + \frac{(\rho\beta)_{nf}}{(\rho\beta)_f} Gr \mathbf{C} \mathbf{v}^n.$$

In above  $\mathbf{A}_{n+1}$ ,  $\mathbf{B}_{n+1}$ ,  $\mathbf{v}_n$ ,  $\mathbf{s}_n^{n+1}$ ,  $\mathbf{C}$  and  $\mathbf{b}^{n+1}$  are represents the block matrices which defined as follow:

$$\begin{aligned}
 \mathbf{A}_{n+1} &= \begin{bmatrix} \mathbf{A}_{n+1}^{\tilde{u}} & \mathbf{0} \\ \mathbf{0} & \mathbf{A}_{n+1}^{\tilde{T}} \end{bmatrix}, \mathbf{B}_{n+1} = \begin{bmatrix} \mathbf{B}_{n+1}^{\tilde{u}} & \mathbf{0} \\ \mathbf{0} & \mathbf{B}_{n+1}^{\tilde{T}} \end{bmatrix}, \mathbf{C} = \begin{bmatrix} \mathbf{0} & \mathbf{I} \\ \mathbf{0} & \mathbf{0} \end{bmatrix}, \mathbf{s}_n^{n+1} = \begin{bmatrix} \mathbf{c}_n^T & \mathbf{0} \\ \mathbf{0} & \mathbf{d}_n^T \end{bmatrix}^{n+1}, \mathbf{v}^n = \\
 \begin{bmatrix} \mathbf{u} \\ \mathbf{T} \end{bmatrix}^n, \mathbf{b}^{n+1} &= \begin{bmatrix} \mathbf{b}_n^T & \mathbf{0} \\ \mathbf{0} & \mathbf{b}_n^T \end{bmatrix}^{n+1},
 \end{aligned}$$

where the matrices  $\mathbf{A}_{n+1}^{\tilde{u}}$ ,  $\mathbf{A}_{n+1}^{\tilde{T}}$ ,  $\mathbf{B}_{n+1}^{\tilde{u}}$ ,  $\mathbf{B}_{n+1}^{\tilde{T}}$ ,  $\mathbf{c}_n^T$ ,  $\mathbf{d}_n^T$ ,  $\mathbf{I}$  and  $\mathbf{b}_n^T$  present in [31] and  $\mathbf{u}$  and  $\mathbf{T}$  are given as:

$$\mathbf{u}^n = [u_1^n, u_2^n, u_3^n, \dots, u_{M-2}^n, u_{M-1}^n]^T,$$

$$\mathbf{T}^n = [T_1^n, T_2^n, T_3^n, \dots, T_{M-2}^n, T_{M-1}^n]^T.$$

#### 4. Results and discussion

This section explore the behavior of non-dimensional velocity and temperature profiles under the influence of the various physical parameters for various values of  $\alpha$ . Figures 1–7 are plotted along with comprehensive discussion for the purpose.

In Figures 1 and 2 are plotted to explain the behavior of velocity of nano- fluid (Copper  $Cu$  and Aluminum oxide  $Al_2O_3$  based) for different values of fractional parameter “ $\alpha$ ” as well as Grashof number “ $Gr$ ”, Hartmann number “ $M$ ”, time “ $t$ ” and solid volume fraction “ $\phi$ ”. Figure 1(a) is plotted against the variation of Grashof number “ $Gr$ ” for the numerous values of “ $\alpha$ ”. It is observed that

velocity profiles demonstrate the increasing behavior with the increase in both Grashof number “Gr” and parameter “ $\alpha$ ”. For the small value of Grashof number the effect of parameter “ $\alpha$ ” is insignificant and vice versa. Effect of Hartman number “ $M$ ” and parameter “ $\alpha$ ” on velocity profile plotted in Figure 1(b). Decreasing behavior of velocity field is detected for different values of Hartmann number “ $M$ ”. This is because the increasing values of Hartmann number “ $M$ ” corresponds the increaser the magnitude of magnetic field. That is why, magnetic forces against the flow process is increasing which become the cause to decrease the velocity of nano- fluid (Copper  $Cu$  and Aluminum oxide  $Al_2O_3$ -based). Behavior of the velocity profile due to the variation in Prandtl number “Pr” and parameter “ $\alpha$ ”. Again similar behavior is achieved under the impact of Prandtl number “Pr” as we got in previous figure that is velocity profiles decreases gradually as Prandtl number “Pr” increases. Dominant effect of parameter “ $\alpha$ ” can be seen for the least value of Prandtl number “Pr”. Effect of time “ $t$ ” and parameter “ $\alpha$ ” analyze in Figure 2(b). Velocity field increases gradually as time increase. Behavior of velocity for different values of fractional parameter “ $\alpha$ ” and solid volume fraction “ $\phi$ ” is present in Figure 3.

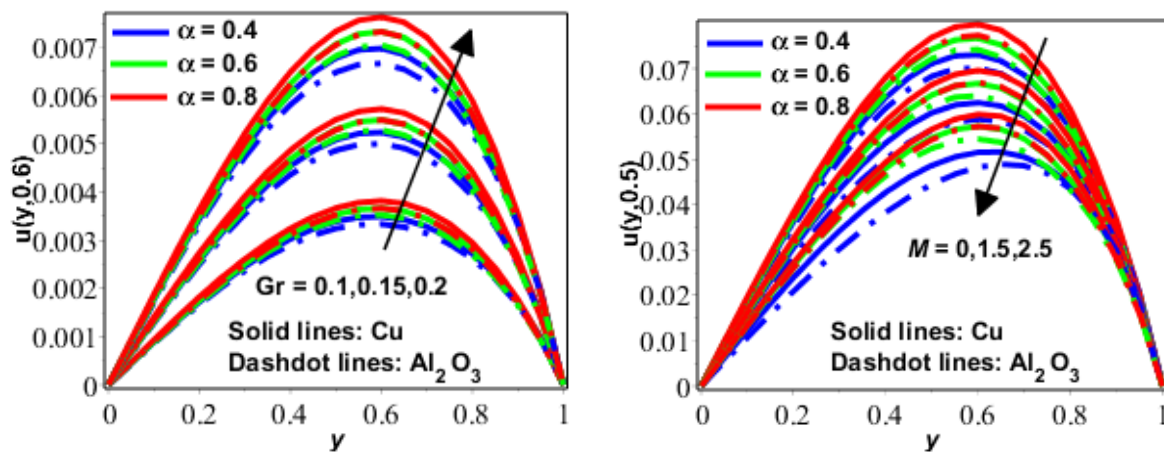


**Figure 1.** Behavior of  $u$  for different values of Gr and  $M$  when  $Pr = 0.7, R = 0.1, M = 1, \phi = 0.1$ .

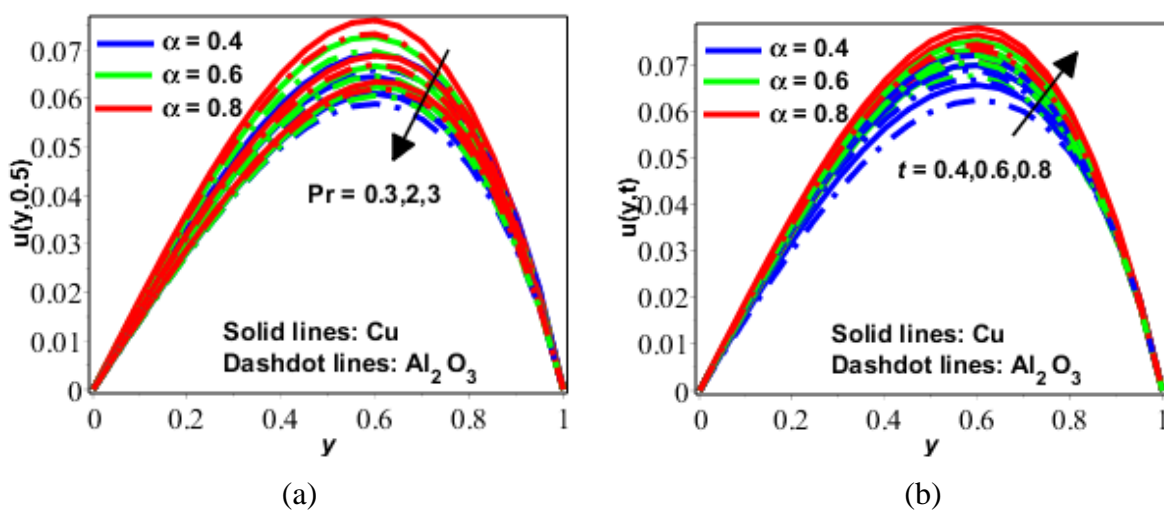


**Figure 2.** (a) Behavior of  $u$  for different values of Pr when  $Gr = 2, R = 1, M = 1, \phi = 0.1$ , (b) Behavior of  $u$  for different values of  $t$  when  $Pr = 0.7, R = 1, Gr = 2, M = 1, \phi = 0.1$ .

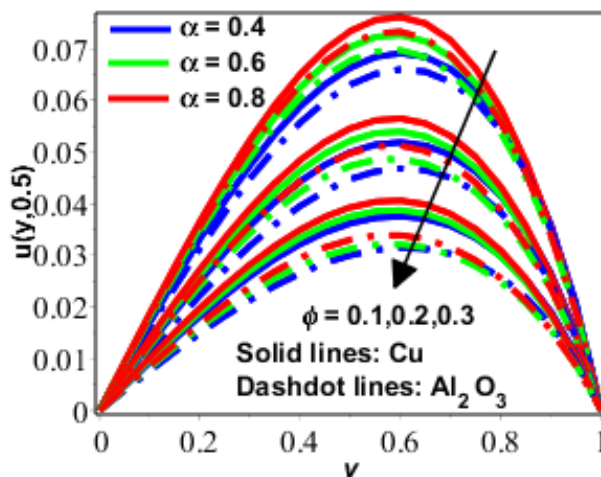


**Figure 3.** Behavior of  $u$  for different values of  $\phi$  when  $Pr = 0.3, R = 1, M = 1, Gr = 2$ .

Observation shows that velocity is decreasing gradually while we are increasing the values of fractional parameter  $\alpha$  and solid volume fraction “ $\phi$ ”. From Figures 1–3, we observed that velocity profiles have dominant values for the case of  $Cu$ -based nanofluid as compare to  $Al_2O_3$ -based nanofluid.

To scrutinize the variation in temperature distribution against the different values of time “ $t$ ”, radiation parameter “ $R$ ”, Prandtl number “ $Pr$ ” and solid volume fraction “ $\phi$ ” Figures 4–8 are portrayed for both Copper ( $Cu$ ) and Aluminum oxide ( $Al_2O_3$ ) based nanofluid.

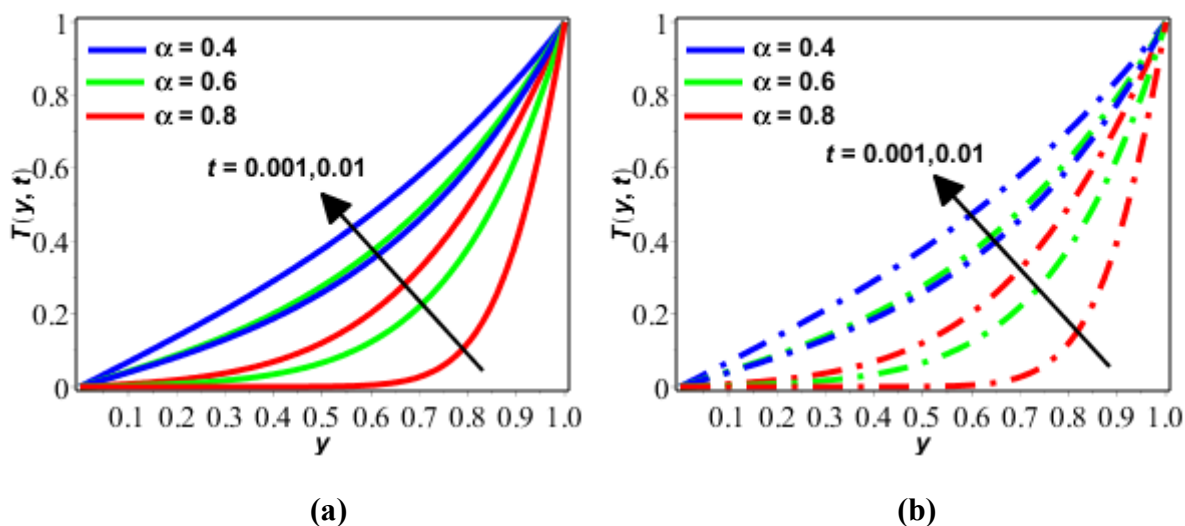


**Figure 4.** Behavior of  $T$  for different values of  $t$  when  $Pr = 0.7, R = 0.1, \phi = 0.1$ .



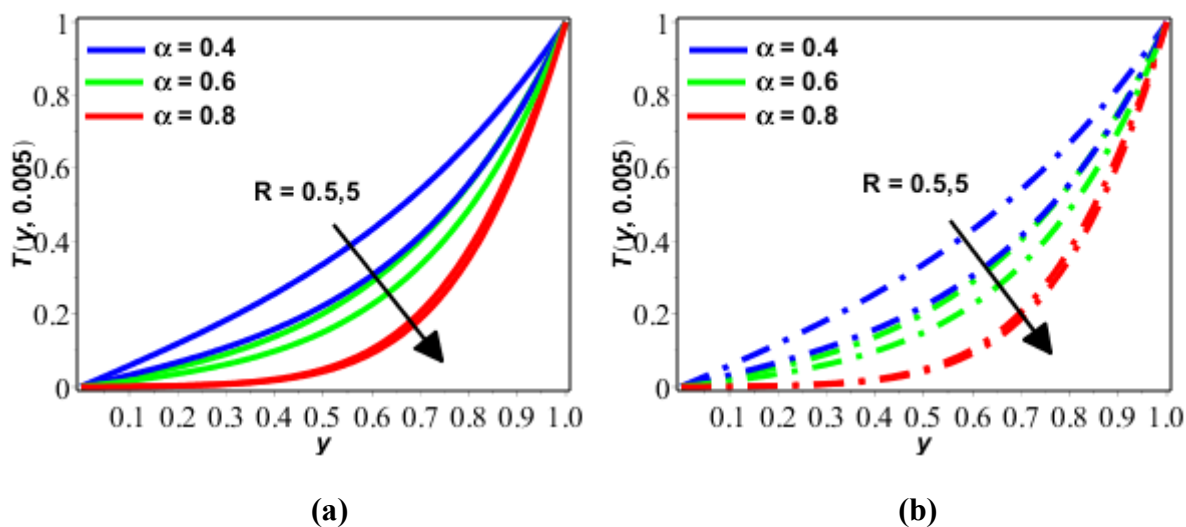


**Figure 5.** Behavior of  $T$  for different values of  $R$  when  $Pr = 0.7, \phi = 0.1$ .

Figure 4 shows the effect of time “ $t$ ” and parameter “ $\alpha$ ” on the temperature field. It is found that temperature profiles increases as upsurge the values of time “ $t$ ”. On the other hand, for the small value of “ $\alpha$ ” behavior of temperature profile is linear. Effect of radiation parameter “ $R$ ” with the numerous values of “ $\alpha$ ” deliberated in Figure 5.

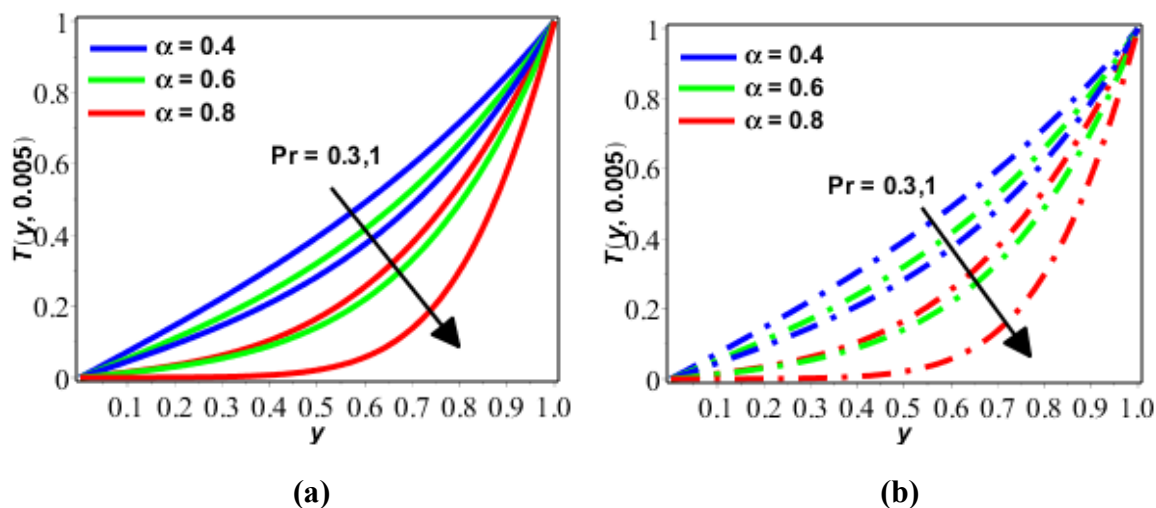


**Figure 6.** Behavior of  $T$  for different values of  $Pr$  when  $R = 1, \phi = 0.1$ .

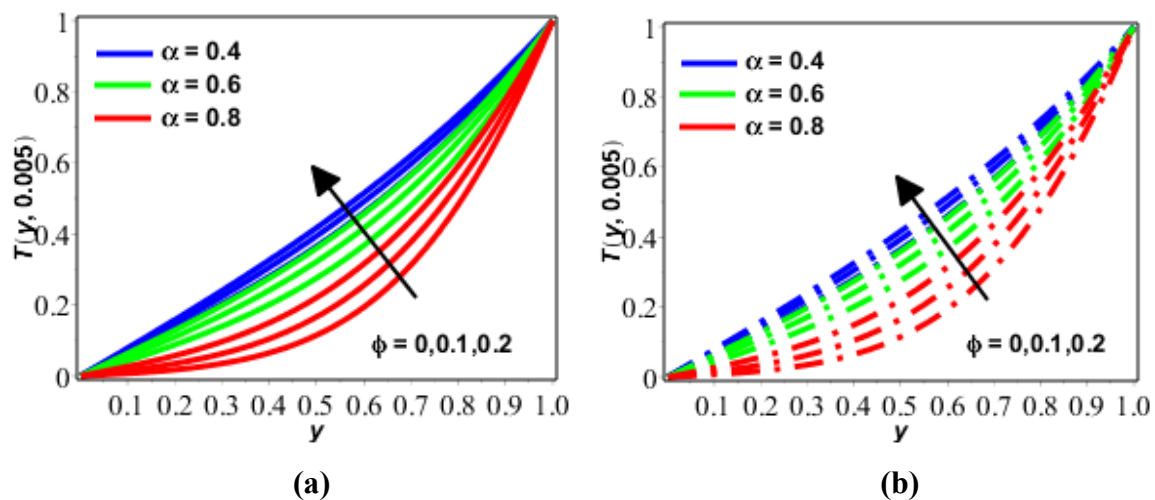


**Figure 7.** Behavior of  $u$  for different values of  $\phi$  when  $Pr = 0.3, R = 1$ .

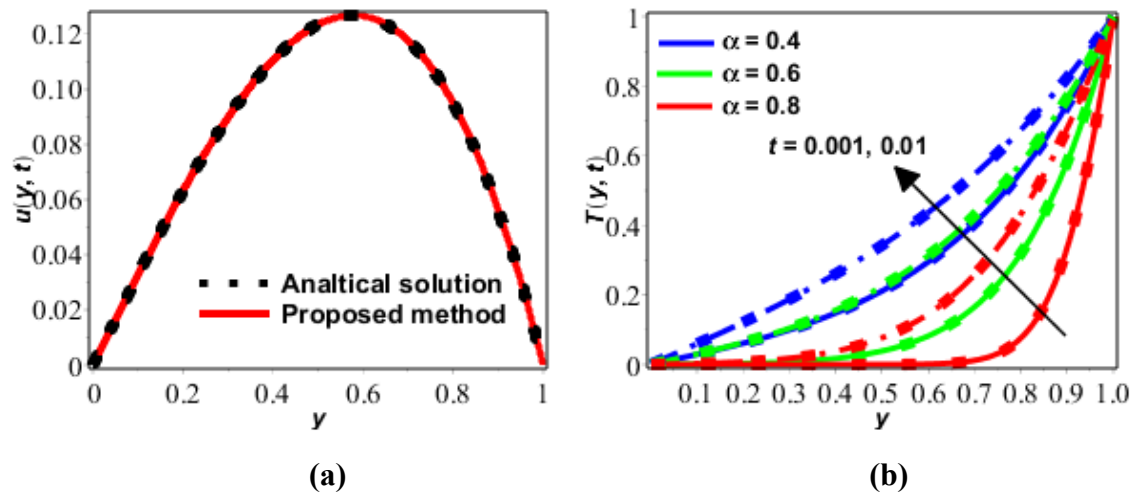


**Figure 8.** Comparison of obtained solutions with existing solutions [30]

Temperature profiles decreases as increasing the radiation parameter. Dominant effect of radiation parameter “ $R$ ” can be seen at the center of channel. Also, temperature increases as parameter “ $\alpha$ ” decreases gradually. Behavior of Prandtl number “ $Pr$ ” and “ $\alpha$ ” on the dimensionless temperature profile demonstrated in Figure 8. Enhancement in Prandtl number decrease the temperature distribution gradually. Lastly, effect of solid volume fraction “ $\phi$ ” and parameter “ $\alpha$ ” on temperature distribution pondered in Figure 7. Here temperature of the fluid enhanced as enhancing both parameters. From Figures 4–7, we observe that temperature profiles have dominant values for the case of  $Cu$ -based nanofluid as compare to  $Al_2O_3$  based nanofluid. Figure 8(a–b) is plotted to demonstrate the comparison of proposed finite difference scheme with published work [30]. Figure 8(a) clearly exhibit that the obtained solutions are excellent agreement with published work. The main advantage of the proposed method that it is accurate and can be extended for nonlinear problem. Figure 8(b) shows the comparison of temperature profile for different values of time and fractional-order parameter  $\alpha$ , it can be noted that for all values of  $\alpha$  and  $t$  the achieved solutions

shows the good agreement with analytical solutions [30]. Table 1 is constructed for the estimation of  $L_2, L_\infty$  and RMS norms using the following relations.

$$E_j = T_j - \tilde{T}_j,$$

$$L_\infty = \max_j |E_j|, L_2 = \sqrt{\sum_{j=1}^M |E_j|^2}, RMS = \sqrt{\frac{1}{M} \sum_{j=1}^M |E_j|^2}.$$

It concluded that proposed method is accurate, stable and well-matched to tackle this problem and also can be extended fractional-order nonlinear problem of physical nature.

**Table 1.** Error analysis of  $L_2, L_\infty$  and RMS using proposed method when  $h = 0.04, k = 0.001$ .

$\alpha$	Norms	$t = 0.1$	$t = 0.5$	$t = 0.9$
0.4	$L_2$	$2.65 \times 10^{-2}$	$3.28 \times 10^{-3}$	$1.50 \times 10^{-3}$
	$L_\infty$	$2.64 \times 10^{-2}$	$3.27 \times 10^{-3}$	$1.49 \times 10^{-3}$
	RMS	$5.90 \times 10^{-3}$	$7.33 \times 10^{-4}$	$3.37 \times 10^{-4}$
0.7	$L_2$	$1.80 \times 10^{-2}$	$1.78 \times 10^{-3}$	$6.45 \times 10^{-4}$
	$L_\infty$	$1.79 \times 10^{-2}$	$1.77 \times 10^{-3}$	$6.44 \times 10^{-4}$
	RMS	$4.02 \times 10^{-3}$	$3.98 \times 10^{-4}$	$1.44 \times 10^{-4}$
1.0	$L_2$	$5.07 \times 10^{-2}$	$3.90 \times 10^{-4}$	$3.82 \times 10^{-5}$
	$L_\infty$	$5.06 \times 10^{-2}$	$3.90 \times 10^{-4}$	$3.82 \times 10^{-5}$
	RMS	$1.13 \times 10^{-2}$	$8.73 \times 10^{-5}$	$8.55 \times 10^{-6}$

## 5. Conclusion

In the presence of magnetic effects, we analyzed the unsteady natural convection radiating flow in an open ended vertical channel. We assumed the channel is stationary with non-uniform temperature. The finite difference approach coupled with Crank Nicolson method has been successfully applied to obtain the solution of said fluid model. Hence, key findings of our study are stated below:

- The temperature decreased due to increase in fractional parameter and radiative parameter  $R$ .
- The temperature increased when we enhanced the value of time.
- The velocity of the fluid decreased while enhancing the radiative parameter  $R$  as well as Prandtl number  $Pr$ .
- The Grashof number  $Gr$  enhanced the velocity of the fluid while fluid velocity decreased with the passage of time  $t$ .
- For lesser values of time  $t$ , while increase in the fractional parameter  $\alpha$  the velocity of the fluid increases but after some critical values of time  $t_c$  the behavior is reverse.

## Acknowledgements

The corresponding author is grateful for the support of Peking University through the Boya Post-doctoral Fellowship. The first author is thankful to Prof. Wei Wang and Chinese scholarship

council for providing him an opportunity to study in China and research-oriented environment.

### Conflict of interest

The authors declare that there is no conflict of interests.

### References

1. T. Fujii, M. Takeuchi, M. Fujii, et al. *Experiments on natural-convection heat transfer from the outer surface of a vertical cylinder to liquids*, Int. J Heat Mass Tran., **13** (1970), 753–787.
2. T. Fujii, H. Imura, *Natural-convection heat transfers from a plate with arbitrary inclination*, Int. J Heat Mass Tran., **15** (1972), 755–767.
3. M. A. Ezzat, *Thermoelectric MHD non-Newtonian fluid with fractional derivative heat transfer*, Physica B, **405** (2010), 4188–4194.
4. M. Arshad, M. H. Inayat, I. R. Chughtai, *Experimental study of natural convection heat transfer from an enclosed assembly of thin vertical cylinders*, Appl. Therm. Eng., **31** (2011), 20–27.
5. N. T. M. Eldabe, S. N. Sallam, M. Y. Abou-zeid, *Numerical study of viscous dissipation effect on free convection heat and mass transfer of MHD non-Newtonian fluid flow through a porous medium*, Journal of the Egyptian mathematical society, **20** (2012), 139–151.
6. Q. Rubbab, D. Vieru, C. Fetecau, et al. *Natural convection flow near a vertical plate that applies a shear stress to a viscous fluid*, PloS one, **8** (2013), e78352.
7. R. Ellahi, *The effects of MHD and temperature dependent viscosity on the flow of non-Newtonian nanofluid in a pipe: analytical solutions*, Appl. Math. Model., **37** (2013): 1451–1467.
8. M. M. Molla, A. Biswas, A. Al-Mamun, et al. *Natural convection flow along an isothermal vertical flat plate with temperature dependent viscosity and heat generation*, Journal of computational engineering, **2014** (2014), 1–13.
9. M. A. Ezzat, A. A. El-Bary, A. S. Hatem, *State space approach to unsteady magnetohydrodynamics natural convection heat and mass transfer through a porous medium saturated with a viscoelastic fluid*, J. Appl. Mech. Tech. Phy., **55** (2014), 660–671.
10. S. R. Sheri, T. Thumma, *Numerical study of heat transfer enhancement in MHD free convection flow over vertical plate utilizing nanofluids*, Ain Shams Eng. J., **9** (2016), 1169–1180.
11. S. Z. Alamri, A. A. Khan, M. Azeez, et al. *Effects of mass transfer on MHD second grade fluid towards stretching cylinder: a novel perspective of Cattaneo–Christov heat flux model*, Phys. Lett. A, **383** (2019), 276–281.
12. F. Ali, M. Saqib, I. Khan, et al. *Application of Caputo-Fabrizio derivatives to MHD free convection flow of generalized Walters’-B fluid model*, Eur. Phys. J. Plus, **131** (2016), 377.
13. M. Hamid, T. Zubair, M. Usman, et al. *Natural convection effects on heat and mass transfer of slip flow of time-dependent Prandtl fluid*, Journal of Computational Design and Engineering, 2019.
14. M. A. Yousif, H. F. Ismael, T. Abbas, et al. *Numerical study of momentum and heat transfer of MHD Carreau nanofluid over an exponentially stretched plate with internal heat source/sink and radiation*, Heat Transf. Res., **50** (2019), 649–658.
15. M. Hamid, M. Usman, R. U. Haq, *Wavelets investigation of Soret and Dufour effects on*

*stagnation point fluid flow in two-dimension with variable thermal conductivity and diffusivity*, Phys. Scripta, 2019.

16. S. U. Choi, J. A. Eastman, *Enhancing thermal conductivity of fluids with nanoparticles*. ASME International Mechanical Engineering Congress & Exposition, 1995.
17. S. U. S Choi, Z. G. Zhang, W. Yu, et al. *Anomalous thermal conductivity enhancement in nanotube suspensions*, Appl. Phys. Lett., **79** (2001), 2252–2254.
18. S. Dinarvand, R. Hosseini, M. Abulhasansari, et al. *Buongiorno's model for double-diffusive mixed convective stagnation-point flow of a nanofluid considering diffusiophoresis effect of binary base fluid*, Adv. Powder Technol., **26** (2015), 1423–1434.
19. M. Sheikholeslami, R. Ellahi, *Three dimensional mesoscopic simulation of magnetic field effect on natural convection of nanofluid*, Int. J. Heat Mass Tran., **89** (2015), 799–808.
20. M. Sheikholeslami, D. D. Ganji, *Nanofluid convective heat transfer using semi analytical and numerical approaches: a review*, J. Taiwan Inst. Chem. E., **65** (2016), 43–77.
21. M. Usman, M. Hamid, U. Khan, et al. *Differential transform method for unsteady nanofluid flow and heat transfer*, Alex. Eng. J., **57** (2018), 1867–1875.
22. M. Hassan, R. Ellahi, M. M. Bhatti, et al. *A comparative study on magnetic and non-magnetic particles in nanofluid propagating over a wedge*. Can. J. Phys., **97** (2019), 277–285.
23. S. T. Mohyud-Din, M. Usman, K. Afaq, et al. *Examination of carbon-water nanofluid flow with thermal radiation under the effect of Marangoni convection*, Eng. Computations, **34** (2017), 2330–2343.
24. M. Hamid, M. Usman, Z. H. Khan, et al. *Numerical study of unsteady MHD flow of Williamson nanofluid in a permeable channel with heat source/sink and thermal radiation*, Eur. Phys. J. Plus, **133** (2018), 527.
25. N. A. Sheikh, F. Ali, M. Saqib, et al. *Comparison and analysis of the Atangana–Baleanu and Caputo–Fabrizio fractional derivatives for generalized Casson fluid model with heat generation and chemical reaction*, Results Phys., **7** (2017), 789–800.
26. M. A. Ezzat, A. A. El-Bary, *MHD free convection flow with fractional heat conduction law*, Magnetohydrodynamics, **48** (2012).
27. F. Ali, N. A. Sheikh, I. Khan, et al. *Magnetic field effect on blood flow of Casson fluid in axisymmetric cylindrical tube: A fractional model*, J. Magn. Magn. Mater., **423** (2017), 327–336.
28. M. A. Imran, I. Khan, M. Ahmad, et al. *Heat and mass transport of differential type fluid with non-integer order time-fractional Caputo derivatives*, J. Mol. Liq., **229** (2017), 67–75.
29. M. Hamid, M. Usman, R. U. Haq, et al. *Wavelets Analysis of Stagnation Point Flow of non-Newtonian Nanofluid*, Appl. Math. Mech.-Engl., **40** (2019), 1211–1226.
30. I. Podlubny, *Fractional differential equations*, Academic press, San Diego, 1999.
31. V. V. Kulish, J. L. Lage, *Application of fractional calculus to fluid mechanics*. J. Fluids Eng.-T. Asme, **124** (2002), 803–806.
32. J. A. T. Machado, M. F. Silva, R. S. Barbosa, et al. *Some applications of fractional calculus in engineering*, Math. Probl. Eng., **2010** (2010), 1–34.
33. T. Pfitzenreiter, *A physical basis for fractional derivatives in constitutive equations*, ZAMM-Zeitschrift für angewandte mathematik und mechanik, **84** (2004), 284–287.
34. Y. Kawada, H. Nagahama, H. Hara, *Irreversible thermodynamic and viscoelastic model for power-law relaxation and attenuation of rocks*, Tectonophysics, **427** (2006), 255–263.

35. M. Usman, M. Hamid, T. Zubair, et al. *Operational-matrix-based algorithm for differential equations of fractional order with Dirichlet boundary conditions*, Eur. Phys. J. Plus, **134** (2019), 279.
36. M. Hamid, M. Usman, T. Zubair, et al. *An efficient analysis for N-soliton, Lump and lump-kink solutions of time-fractional (2+1)-Kadomtsev–Petviashvili equation*, Physica A, **528** (2019), 121320.
37. N. A. Shah, D. Vieru, C. Fetecau, *Effects of the fractional order and magnetic field on the blood flow in cylindrical domains*, J. Magn. Magn. Mater., **409** (2016), 10–19.
38. M. A. Ezzat, I. A. Abbas, A. A. El-Bary, et al. *Numerical study of the Stokes' first problem for thermoelectric micropolar fluid with fractional derivative heat transfer*, Magnetohydrodynamics, **50** (2014).
39. I. Khan, N. A. Shah, Y. Mahsud, et al. *Heat transfer analysis in a Maxwell fluid over an oscillating vertical plate using fractional Caputo-Fabrizio derivatives*, Eur. Phys. J. Plus, **132** (2017), 194.
40. B. Ahmad, S. I. Shah, S. U. Haq, et al. *Analysis of unsteady natural convective radiating gas flow in a vertical channel by employing the Caputo time-fractional derivative*, Eur. Phys. J. Plus, **132** (2017), 380.
41. H. Sun, W. Chen, C. Li, et al. *Finite difference schemes for variable-order time fractional diffusion equation*, Int. J. Bifurcat. Chaos, **22** (2012), 1250085.
42. C. Çelik, M. Duman, *Crank–Nicolson method for the fractional diffusion equation with the Riesz fractional derivative*, J. Comput. Phys., **231** (2012), 1743–1750.
43. A. C. Cogley, W. G. Vincenti and S. E. Gilles, *Differential Approximation for Radiative Transfer in a Non-Grey Gas near Equilibrium*, AIAA J., **6** (1968), 551–553.



AIMS Press

© 2019 the Author(s), licensee AIMS Press. This is an open access article distributed under the terms of the Creative Commons Attribution License (<http://creativecommons.org/licenses/by/4.0>)